

Implication of odd-even staggering in the charge radii of calcium isotopes

Rong An,^{1,2} Xiang Jiang,³ Na Tang,^{1,2} Li-Gang Cao,^{2,4,*} and Feng-Shou Zhang^{2,4,5,†}

¹*School of Physics, Ningxia University, Yinchuan 750021, China*

²*Key Laboratory of Beam Technology of Ministry of Education,*

College of Nuclear Science and Technology, Beijing Normal University, Beijing 100875, China

³*College of Physics and Optoelectronic Engineering, Shenzhen University, Shenzhen 518060, China*

⁴*Key Laboratory of Beam Technology of Ministry of Education, Institute of Radiation Technology, Beijing Academy of Science and Technology, Beijing 100875, China*

⁵*Center of Theoretical Nuclear Physics, National Laboratory of Heavy Ion Accelerator of Lanzhou, Lanzhou 730000, China*

(Dated: April 30, 2024)

Inspired by the evidently observed odd-even staggering and the inverted parabolic-like shape of charge radii along calcium isotopic chain, the ground state properties of calcium isotopes are investigated by constraining the root-mean-square (rms) charge radii under the covariant energy density functionals with effective forces NL3 and PK1. In this work, the pairing correlations are tackled by solving the state-dependent Bardeen-Cooper-Schrieffer equations. The calculated results suggest that the binding energies obtained by constraint method have been reduced less than 0.1%. But for charge radii, the corresponding results deriving from NL3 and PK1 forces have been increased by about 1.0% and 2.0%, respectively. This means that charge radius is a more sensitive quantity in the calibrated protocol. Meanwhile, it is found that the reproduced charge radii of calcium isotopes is attributed to the rather strong isospin dependence of effective potential. The odd-even oscillation behavior can also be presented in the neutron skin thickness and proton Fermi energy along calcium isotopic chain, but keep opposite trends with respect to the corresponding binding energy and charge radius. As encountered in charge radii, the weakening odd-even oscillation behavior is still emerged from the proton Fermi energies at the neutron numbers $N = 20$ and 28 as well, but not in binding energy and neutron skin thickness.

I. INTRODUCTION

Accurate description of nuclear charge radii deriving from charge density distributions plays an important role in theoretical studies. It is due to the fact that the fine structure of nuclear size can encode the information about the shape-phase transition [1–9], halo structure [10, 11], and the emergence of magic numbers [12, 13], etc. Also, recent studies suggest that charge radii of mirror partner nuclei can provide an alternative access to probe the equation of state (EoS) of isospin asymmetric nuclear matter [14–24]. With the advent of radioactive beam facilities, more database about charge radii are compiled [25, 26]. Thus this challenges us to recognize the fine structure of atomic nuclei with high-precision in nuclear models.

The global features of nuclear charge radii can be generally described by the $A^{1/3}$ or $Z^{1/3}$ law [27, 28], with A and Z the mass and proton numbers. However, these empirical formulae are not valid any more for nuclei with larger ratio of neutron to proton. In addition, it is difficult to inspect the microscopic implications, e.g., the proton and neutron density distributions. The same scenarios can also be encountered in the Bayesian neural networks [29, 30], in which the microscopic aspects cannot be completely captured and the extrapolating ability is restricted due to the limited databases. Along a long

isotopic chain, the evolution of nuclear charge radii has performed regularity and irregularity behaviors [31, 32]. Especially in calcium isotopes, the inverted parabolic-like shape and strong odd-even oscillations in charge radii can be apparently observed between ^{40}Ca and ^{48}Ca isotopes [25]. Also, such peculiar feature of the strong odd-even oscillations in charge radii persists toward the neutron-deficient region [33]. It is also mentioned that the databases of charge radii for ^{40}Ca (3.4776 fm) and ^{48}Ca (3.4777 fm) isotopes are almost equivalent, and the shell quenching effect in charge radii has been observed at the neutron number $N = 28$ but not at $N = 20$. Across the ^{48}Ca isotope, the rapid increase of charge radii is performed until to ^{52}Ca . The values of charge radii for ^{44}Ca (3.5188 fm) and ^{50}Ca (3.5192 fm) are also visually identical [25, 26]. For ^{52}Ca , as a candidate of doubly magic nuclei [34–37], the shell quenching in charge radii cannot be expected naturally [38]. These particular features can provide insights into the underlying mechanism in theoretical researches.

Plenty of methods have been undertaken to elucidate the global trend of charge radii tentatively along calcium isotopes. *Ab initio* calculations with chiral effective field theory interactions, such as NNLOsat [39] with SRG1 and SRG2 interactions [40], cannot reproduce the discontinuous changes of charge radii along calcium isotopes well [38]. The major classes of covariant energy density functionals (CEDFs) have made greatly success in describing the ground state properties of finite nuclei over the whole periodic table [41–44]. However, the description and explanation for some fine structures, such as the odd-even staggering (OES) of charge radii in calcium iso-

* Corresponding author: caolg@bnu.edu.cn

† Corresponding author: fszhang@bnu.edu.cn

topes, are still not adequate yet. As shown in Ref. [45], the effect of short-rang correlations has an influence on the charge radii and nuclear Fermi surface. Miller, *et al.* further point out that neutron-proton short-range correlations can have an influence on determining the nuclear charge radius [46]. The short-range correlation between neutron and proton implies the fluctuation of occupation for the states around Fermi surface [47]. This suggests that more isospin interactions should be taken into account in describing the nuclear size [48]. In Ref. [49], a novel ansatz has been added into the root-mean-square (rms) charge radii formula. This modified expression can reproduce the trend of changes in charge radii and OES well, and this accounts for the correlations between the neutron and proton pairs around Fermi surface [50, 51]. In the Fayans energy density functional model, these local variations are attributed to the surface pairing interactions [52]. In order to inspect the anomalous behaviors in the charge radii of calcium isotopes, the further research should be performed at the mean field level.

In this work, we put emphasis on the possibly microscopic mechanisms of such enhancement OES and the inverted parabolic-like shape in charge radii of calcium isotopes. To facilitate the underlying mechanism of OES in nuclear size, the constraint calculations on the root-mean-square (rms) charge radii are performed along calcium isotopes. The binding energies obtained by constraint calculations are also examined. Meanwhile, we further review the evolution of the neutron and proton Fermi energies along the neutron number excess. The inverse odd-even oscillation of proton Fermi energy is shown against the OES of charge radii in calcium isotopes. The neutron Fermi surface along a long isotopic chain is almost not changed before and after making constraint, but the inverse OES in neutron-skin thickness is found dramatically.

The structure of the paper is organized as the follows. Sec. II is devoted to presenting the theoretical framework briefly. In Sec. III, the numerical results and discussion are provided. Finally, a summary and outlook is given in Sec. IV.

II. THEORETICAL FRAMEWORK

The covariant energy density functionals (CEDFs) have been widely used to investigate various physical phenomena, such as halo structure [53–57], pseudospin symmetry [58–60], hypernuclei [61], effect of resonant [62–67], location of dripline [68–70], nuclear fission [71, 72], and neutron drops [73], etc. In this work, the non-linear self-coupling Lagrangian density is employed [74], where the constituent nucleons are described as Dirac particles which interact via the exchange of σ , ω and ρ mesons. The electromagnetic field is mediated by photons. Since

the effective Lagrangian density is recalled as follows,

$$\begin{aligned} \mathcal{L} = & \bar{\psi}[i\gamma^\mu\partial_\mu - M - g_\sigma\sigma - \gamma^\mu(g_\omega\omega_\mu + g_\rho\vec{\tau}\cdot\vec{\rho}_\mu + e\frac{1-\tau_3}{2}A_\mu)]\psi \\ & + \frac{1}{2}\partial^\mu\sigma\partial_\mu\sigma - \frac{1}{2}m_\sigma^2\sigma^2 - \frac{1}{3}g_2\sigma^3 - \frac{1}{4}g_3\sigma^4 \\ & - \frac{1}{4}\Omega^{\mu\nu}\Omega_{\mu\nu} + \frac{1}{2}m_\omega^2\omega_\mu\omega^\mu + \frac{1}{4}c_3(\omega^\mu\omega_\mu)^2 \\ & - \frac{1}{4}\vec{R}_{\mu\nu}\cdot\vec{R}^{\mu\nu} + \frac{1}{2}m_\rho^2\vec{\rho}^\mu\cdot\vec{\rho}_\mu + \frac{1}{4}d_3(\vec{\rho}^\mu\vec{\rho}_\mu)^2 \\ & - \frac{1}{4}F^{\mu\nu}F_{\mu\nu}, \end{aligned} \quad (1)$$

where M is the mass of nucleon and m_σ , m_ω , and m_ρ , are the masses of the σ , ω and ρ mesons, respectively. Here, g_σ , g_ω , g_ρ , g_2 , g_3 , c_3 and d_3 are the coupling constants for σ , ω and ρ mesons, respectively, while $e^2/4\pi = 1/137$ is the fine structure constant. The field tensors for the vector mesons and photon fields are defined as $\Omega_{\mu\nu} = \partial_\mu\omega_\nu - \partial_\nu\omega_\mu$, $\vec{R}_{\mu\nu} = \partial_\mu\vec{\rho}_\nu - \partial_\nu\vec{\rho}_\mu - g_\rho(\vec{\rho}_\mu \times \vec{\rho}_\nu)$ and $F_{\mu\nu} = \partial_\mu A_\nu - \partial_\nu A_\mu$.

The Dirac equations derived from the variational principle can be expressed as follows,

$$\mathcal{H} = -i\alpha\nabla + V(\mathbf{r}) + \beta[M + S(\mathbf{r})], \quad (2)$$

where $S(\mathbf{r})$ and $V(\mathbf{r})$ represent the effective fields [74]. The bulk properties of finite nuclei are calculated by the effective forces NL3 [75] and PK1 [76].

As mentioned before, the discontinuous behavior of charge radii along calcium isotopes cannot be reproduced well by the relativistic mean field calculations. To further review the microscopic mechanism in reproducing the OES of charge radii along calcium isotopes, we make a constraint calculations on the rms charge radii. Therefore, the Hamiltonian can be rewritten as the following expression,

$$\mathcal{H}' = \mathcal{H} - \lambda\langle R_{\text{ch}} \rangle, \quad (3)$$

where λ is the spring constant. The quantity of $\langle R_{\text{ch}} \rangle$ can be calculated through (in units of fm²)

$$R_{\text{ch}}^2 = \langle r_p^2 \rangle + 0.64 \text{ fm}^2. \quad (4)$$

The first term represents the charge density distributions of point-like protons and the second term is due to the finite size of protons [77]. The accuracy of the convergence is determined by the self-consistent iteration in binding energy, which is lower than 10^{-6} MeV.

III. RESULTS AND DISCUSSION

At the mean field level, the bulk properties of finite nuclei can be described well [78, 79]. While more possible mechanisms are urgently required to comprehend these anomalous behaviors in nuclear charge radii. In this work, the global trend of nuclear charge radii along calcium isotopic chain is discussed thereby the constraint calculations on nuclear size. The pairing correlations

can be treated by solving the state-dependent Bardeen-Cooper-Schrieffer (BCS) equations which can describe the ground state properties of finite nuclei well [41]. The pairing strength is chosen to be $V_0 = 350 \text{ MeV fm}^3$ for NL3 force, but $V_0 = 380 \text{ MeV fm}^3$ for PK1 parametrization set. The calculated results show that the quadrupole deformation of calcium isotopes cannot be changed with and without considering constraint, namely keep almost spherical shape.

In our calculations, the binding energies obtained by constraint method has been reduced less than 0.1% for NL3 set and about 0.1% for PK1 set. However, for charge radii, the constraint results obtained by NL3 effective force has been increased about 1%, but about 2% for PK1 force. This difference is due to the fact that the effective force NL3 can almost reproduce the charge radii of ^{40}Ca (3.4692 fm) and ^{48}Ca (3.4711 fm) isotopes without considering constraint calculation on charge radius, but apparent discrepancy occurs for PK1 set, namely 3.4445 fm for ^{40}Ca and 3.4542 fm for ^{48}Ca . This leads to the systematically underestimated results in charge radii for effective force PK1 [49]. Furthermore, these results suggest that charge radii are more sensitive quantities in the calibrated protocol. This seems to provide a guideline to the artificial neural networks in learning experimental data.

The odd-even staggering behaviors in charge radii and nuclear mass are generally observed throughout the whole nuclear chart [25, 26, 80]. To facilitate these local phenomena, the three-point formula is recalled as follows,

$$\Delta_{\mathcal{Y}}(N, Z) = \frac{1}{2}[2\mathcal{Y}(N, Z) - \mathcal{Y}(N-1, Z) - \mathcal{Y}(N+1, Z)], \quad (5)$$

where $\mathcal{Y}(N, Z)$ represents the specific physical quantity of a nucleus with neutron number N and proton number Z .

In Fig. 1, the OES of binding energy and charge radii are calculated by Eq. (5), respectively. As shown in Fig. 1 (a) and (c), here one can find that the OES of nuclear mass evaluated theoretically agrees with the experimental data very well. With and without considering the constraint on rms charge radii, the OES of binding energy obtained by both methods can give almost similar trend. In addition, one can find that the amplitudes of OES in binding energies are enlarged at the neutron numbers $N = 20$ and $N = 28$ with respect to the neighboring nuclei. This emerging signature of changes in shell gap could be generally used to identify the new magic numbers [80].

In Fig. 1 (b) and (d), OES of rms charge radii is plotted as a function of neutron number with effective forces NL3 and PK1. As discussed in Ref. [49], the local variations of charge radii cannot be reproduced well under the relativistic mean field model with Eq. (4). Especially, the underestimated OES behaviors are obtained by these NL3 and PK1 forces. Because of the constraint calculations on rms charge radii, the calculated results can spontaneously cover the experimental databases. The OES of

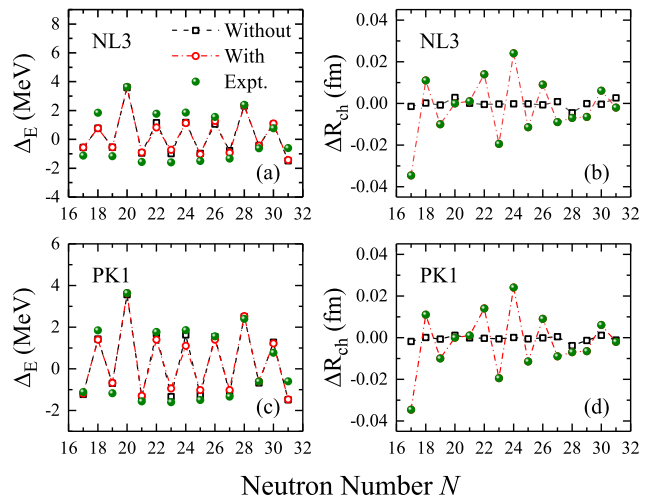


FIG. 1. (Color online) Odd-even staggering of binding energy and root-mean-square (rms) charge radii of calcium isotopes as a function of neutron number are depicted by both NL3 (a, b) and PK1 (c, d) effective forces. The corresponding experimental data are taken from Refs. [25, 26, 80].

charge radii between the neutron numbers $N = 20$ and $N = 28$ are dramatically observed under constraint calculation. As shown in Fig. 1 (a) and (c), the enlarged OES in binding energy results from the strong shell closure. However, the odd-even oscillation amplitudes of charge radii are weakened at the $N = 20$ and $N = 28$ shell closure. As demonstrated in Ref. [50], the weakening OES behavior of nuclear charge radii is observed generally at the strong shell closure. This may provide a signature to feature the magicity of a nucleus from the aspect of nuclear size. As a candidate of doubly magic nuclei, the unexpectedly larger charge radius has been observed in ^{52}Ca [38]. Thus the charge radius of ^{53}Ca isotope is urgently required. The latest study suggests that the shell quenching of nuclear charge radii along Sc isotopic chain can be observed notably at the neutron number $N = 20$ [81]. But this phenomenon is absent in the neighboring Ca isotopes.

The pairing interactions can dominate the anomalous behavior of charge radii along calcium isotopic chain [52]. Therefore, it is necessary to depict the neutron pairing energy of calcium isotopes with both of the different approaches. In Fig. 2, we show the neutron pairing energy of $^{42-46}\text{Ca}$ isotopes obtained by both methods with and without considering constraint on rms charge radii. For NL3 force, the magnitude of variation is enlarged by making constraint calculation. But for PK1 case, the quantity of neutron pairing energies of $^{42-46}\text{Ca}$ isotopes is almost not changed by these two methods.

The quantity of neutron skin thickness (NST) $\Delta R_{\text{np}} = \sqrt{\langle r_n^2 \rangle} - \sqrt{\langle r_p^2 \rangle}$, which is characterized as the difference between the neutron and proton density distributions in a heavy nucleus, provides a sensitive probe to constrain

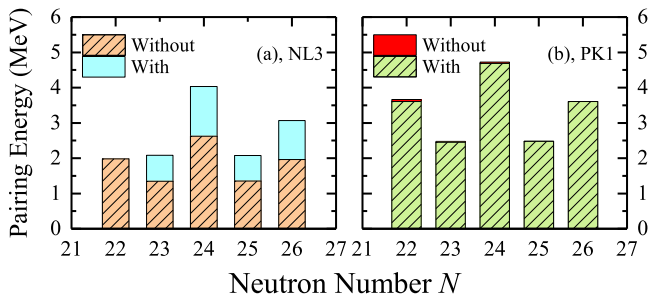


FIG. 2. (Color online) Neutron pairing energy of $^{42-46}\text{Ca}$ isotopes obtained by methods with and without considering constraint on rms charge radii is depicted by NL3 (a) and PK1 forces (b).

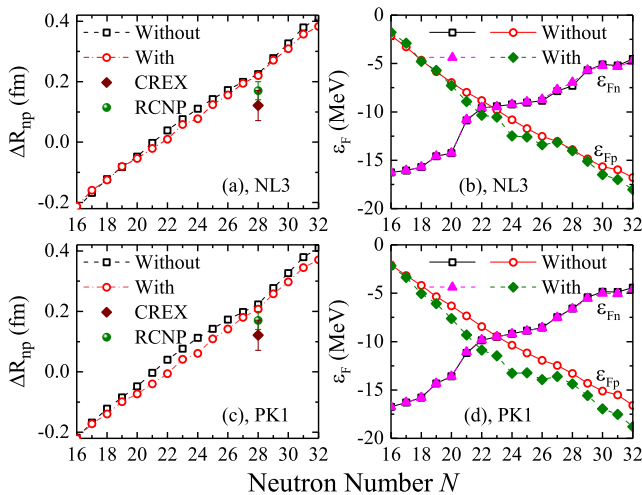


FIG. 3. (Color online) Neutron skin thickness (NST) of calcium isotopes with and without making constraint on the rms charge radius is depicted as a function of neutron number with effective forces NL3 (a) and PK1 (c). The NST of ^{48}Ca obtained through the RCNP [82] and CREX [83] collaborations are also shown for comparison. The Fermi energies of neutron (ε_{Fn}) and proton (ε_{Fp}) are presented in the panel (b) and (d) as well.

the equation of state of isospin asymmetric nuclear matter [84–91]. As shown in Fig. 3 (a) and (c), the isospin dependence of NST is depicted, where the neutron skin is monotonically increased with the increasing neutron numbers N . Without considering the constraint calculations, the thick neutron skins are obtained between $N = 20$ and $N = 28$ due to the underestimated values of charge radii, namely the shrunk proton density distributions. The same scenarios are also occurred beyond ^{49}Ca . By contrast, the constraining results reduce the values of NST for $^{41-47,49,50}\text{Ca}$ isotopes. With increasing neutron number, the quantity of NST is gradually increased as well.

As suggested in Refs. [18, 92–95], the proton and neutron distributions radii depend almost linear on neutron

excess. As shown in Fig. 3 (a) and (c), before making constraint calculation, this linear correlation is disturbed heavily by shell closure effect at $N = 28$. That is why the rapid increase of NST can be observed across the neutron number $N = 28$. In constraining results, this trend is weakened, namely the NST of calcium isotopes is almost linearly increased with the increasing neutron number excess. Comparison of the calculated results for the NST of ^{48}Ca with those from the RCNP [82] and CREX [83] collaborations are also shown. Although NL3 effective force can reproduce the charge radii of ^{48}Ca well, the NST of ^{48}Ca is still overestimated. But for PK1 force, the calculated result is more close to RCNP with respect to CREX. Our calculations can cover the uncertainty range of Ref. [17] where the predicted NST for ^{48}Ca is 0.15-0.21 fm. As demonstrated above, systematic trend of nuclear charge radii along a long isotopic chain can be used to reveal the emergence of neutron magic numbers. Here it suggests that the neutron skin thickness depends almost linear on neutron excess if the constraint calculation is performed carefully.

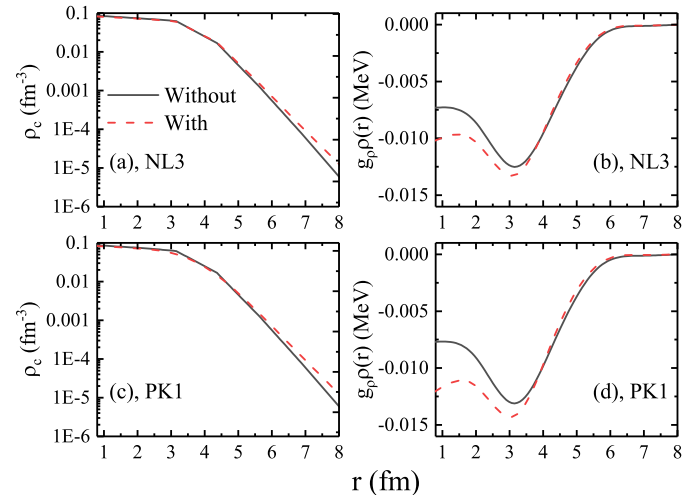


FIG. 4. (Color online) The charge density ρ_c and equivalent ρ meson field $g_\rho\rho(\mathbf{r})$ in ^{44}Ca are depicted by the effective forces NL3 (a, b) and PK1 (c, d).

The neutron skin thickness is related to the disparity of the Fermi energies between proton and neutron in mean-field calculations [96]. In addition, charge radii can be influenced by the nuclear Fermi surface as well [45, 97]. Therefore, it is instructive to present the Fermi energies of neutron (ε_{Fn}) and proton (ε_{Fp}) along calcium isotopes in Fig. 3 (b) and (d). It is mentioned that the neutron Fermi energies are almost not changed under the constraint calculations. But for proton Fermi energies, the apparent divergence occurs between the $N = 20$ and $N = 28$ filled shells. Beyond $N = 29$, this divergence is also presence. This conclusion is in accord with the values of NST where proton and neutron density distributions actually have an influence on Fermi energies. The Fermi energy difference between neutron and proton is associ-

ated with the nuclear symmetry energy [98, 99]. This suggests that the OES in charge radii should be reproduced well by adjusting the associated isospin interactions. It is notably mentioned that the trend of changes of charge radii is influenced by the isospin dependence of the spin-orbit force [100, 101].

In Fig. 4 (a) and (c), the charge density distributions $\rho_c(\mathbf{r})$ of ^{44}Ca are shown with effective forces NL3 and PK1. The constraining results give the relatively larger density distributions in the outer edge ($r > 6$ fm). This leads to that the corresponding central density is reduced naturally. Shown in Ref. [46], it points out that the short-range neutron-proton tensor interaction causes the increasing charge radius, namely exists more strong isospin interactions. Under the relativistic mean field model, the ρ meson is employed to describe the isospin asymmetry degrees. In Fig. 4 (b) and (d), the equivalent meson fields $g_\rho\rho(\mathbf{r})$ in ^{44}Ca are also presented. It shows that the constraining calculations give more bound interaction, namely rather strong isospin couplings. As demonstrated in Ref. [100], the entire isospin dependence of the spin-orbit field is rather small in relativistic calculations. That is why the charge radii of $^{42-46}\text{Ca}$ isotopes cannot be reproduced well in relativistic mean field model. Therefore, the isospin interaction components in effective nuclear potentials should be considered carefully.

Actually, a strong coupling between neutron- and proton-pairing correlations leads to the anomalous behaviors in nuclear charge radii [102]. Furthermore, recent studies suggest that α -cluster structure has been performed in light or medium mass nuclei [103–107]. This means the more strong isospin interactions deriving from the neutron and proton pairs condensation should be taken into account in discussing the fine structure of finite nuclei. Along calcium isotopic chain, the OES behavior in charge radii can be evidently observed. As shown in Fig 3, this anomalous behavior results from the changes of the proton Fermi surface. It seems to propose that the isospin interactions should be reinforced due to the neutron- and proton- pairs condensation.

As encountered in proton Fermi energy, the constraint calculation makes the single-particle levels of protons bound deeply. Such as ^{44}Ca , the constraining result obtained by NL3 force gives the single-particle energy -14.542 MeV for $2s_{1/2}$ orbit. For no constraint result, the single-particle energy of $2s_{1/2}$ orbit is -12.647 MeV. As shown in Fig. 3 (b) and (d), the proton Fermi energy decreases with the increasing isospin asymmetry. The constraining results reproduce the enlarged rms charge radius between ^{40}Ca and ^{48}Ca . Meanwhile, the corresponding proton Fermi energy becomes lower in comparison with the case without making constraint. This may suggest that the isospin interactions in mean-field model or the underlying mechanism resulting from the strong isospin coupling cannot be captured adequately.

The odd-even oscillations behaviors of NST and Fermi energies of proton can be observed apparently. In order to inspect these local variations of NST and the proton

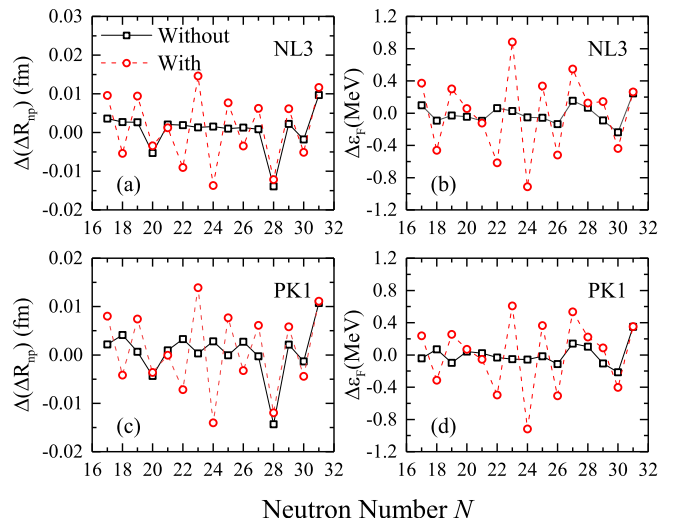


FIG. 5. (Color online) Odd-even oscillations of neutron skin thickness (a, c) and proton Fermi energy (b, d) against calcium isotopes as a function of neutron numbers with effective forces NL3 (a, b) and PK1 (c, d).

Fermi energy, Eq. (5) is still employed to facilitate these discontinuous behaviors. In Fig. 5, the NST of $^{36-52}\text{Ca}$ isotopes and the proton Fermi energy are depicted with NL3 and PK1 forces, respectively. From this figure, we can find that the NST represents the inverse odd-even oscillations in comparison with the corresponding binding energy and charge radii. The same scenarios can also be found in the proton Fermi energies with the increasing neutron numbers. However, the OES behaviors of the proton Fermi energies are weakened at the neutron numbers $N = 20$ and 28 under the NL3 effective force. The same scenario can be found in the PK1 set as well. As demonstrated in Ref. [50], the weakening OES behaviors can be observed in nuclear charge radii due to the strong shell closure effect. This may result from the weakening OES of the proton Fermi energy at the completely filled shells.

IV. SUMMARY AND OUTLOOK

Complementary to the analyses of OES in charge radii along calcium isotopes, the constraint calculations on charge radii are performed. The calculated results suggest that the OES of binding energies are almost similar with these two approaches, and against the experimental database well. The weakening OES of charge radii can be regarded as local irregularity along calcium isotopic chain at neutron numbers $N = 20$ and 28 . This provides a signature to identify the shell closure [31, 50]. The direct determination of the NST usually involves the precise measurement of the root mean square (rms) radii of charge density distributions. Therefore, the NSTs of calcium isotopes are also performed in this work. The

NSTs of calcium isotopes are almost linearly increased with the increasing neutron numbers. Without considering the constraint calculations, the shell effect distorts the linear change of NST heavily, e.g., the apparently shrunk trend occurs at the neutron number $N = 28$.

In order to review the OES behaviors in charge radii, the local variations of NST and the proton Fermi energies for calcium isotopes are delineated by three-point formula Eq. (5). It is obviously mentioned that the OES in the NST and proton Fermi energies show the inverse amplitudes with respect to binding energies and charge radii. Meanwhile, the abnormal OES behaviors can also be found in the Fermi energies at $N = 20$ and 28. This phenomenon cannot be found in the neutron skin thickness. As demonstrated in Refs. [96, 97], the nuclear size can be affected by the Fermi surface or the single-particle orbitals near the Fermi surface. Hence this may offer an explanation why the enhanced odd-even oscillations of charge radii can be observed between ^{40}Ca and ^{48}Ca .

The charge radii of calcium isotopes can be reproduced well by the constraint calculations. The calculated results suggest that the suitable isospin interactions should be supplied in relativistic mean field model. Actually, nuclear charge radii are influenced by various mechanisms, such as high order moment [108, 109], isospin symmetry breaking [110, 111], pairing correlations [112, 113], quadrupole deformation [114], etc. Precision determination of charge radii play a crucial role in nuclear physics.

The linear correlations between the charge radii differences of mirror-pair nuclei and the slope parameter of symmetry energy have been built to ascertain the isospin components of asymmetric nuclear matter interactions. As shown in Refs. [18, 95, 115], the proton radii of mirror-pair nuclei can provide the opportunity to encode the information about neutron skin thickness. This means that the neutron skin thickness and charge radii are mutually determined. Thus, this challenges the nuclear models to perform high-precision descriptions of charge radii of unstable nuclei.

ACKNOWLEDGEMENTS

This work was supported by the National Key R&D Program of China under Grant No. 2023YFA1606401 and the National Natural Science Foundation of China under Grants No. 12047513, No. 12135004, No. 11635003, No. 11961141004, No. 11025524, No. 11161130520, the National Basic Research Program of China under Grant No. 2010CB832903. X. J. was grateful for the support of the National Natural Science Foundation of China under Grants No. 11705118. L.-G. C. was grateful for the support of the National Natural Science Foundation of China under Grants No. 12275025, No. 11975096 and the Fundamental Research Funds for the Central Universities (2020NTST06).

-
- [1] J. Jänecke and F. D. Becchetti, *Phys. Rev. C* **27**, 2282 (1983).
- [2] R. F. Casten, *Phys. Rev. Lett.* **54**, 1991 (1985).
- [3] G. A. Lalazissis, M. M. Sharma, and P. Ring, *Nucl. Phys. A* **597**, 35 (1996).
- [4] R. Rodriguez-Guzman, P. Sarriguren, and L. M. Robledo, *Phys. Rev. C* **82**, 061302(R) (2010).
- [5] T. Togashi, Y. Tsunoda, T. Otsuka, and N. Shimizu, *Phys. Rev. Lett.* **117**, 172502 (2016).
- [6] B. A. Marsh, T. Day Goodacre, S. Sels, Y. Tsunoda, B. Andel, A. N. Andreyev, N. A. Althubiti, D. Atanasov, A. E. Barzakh, J. Billowes, K. Blaum, T. E. Cocolios, J. G. Cubiss, J. Dobaczewski, G. J. Farooq-Smith, D. V. Fedorov, V. N. Fedosseev, K. T. Flanagan, L. P. Gaffney, L. Ghys, M. Huyse, S. Kreim, D. Lunney, K. M. Lynch, V. Manea, Y. Martinez Palenzuela, P. L. Molkanov, T. Otsuka, A. Pastore, M. Rosenbusch, R. E. Rossel, S. Rothe, L. Schweikhard, M. D. Seliverstov, P. Spagnoletti, C. Van Beveren, P. Van Duppen, M. Veinhard, E. Verstraelen, A. Welker, K. Wendt, F. Wienholtz, R. N. Wolf, A. Zadornaya, and K. Zuber, *Nature Phys.* **14**, 1163 (2018).
- [7] A. Barzakh, A. N. Andreyev, C. Raison, J. G. Cubiss, P. Van Duppen, S. Péru, S. Hilaire, S. Goriely, B. Andel, S. Antalic, M. Al Monthery, J. C. Berengut, J. Bieroń, M. L. Bissell, A. Borschevsky, K. Chrysalidis, T. E. Cocolios, T. Day Goodacre, J.-P. Dognon, M. Elantkowska, E. Eliav, G. J. Farooq-Smith, D. V. Fedorov, V. N. Fedosseev, L. P. Gaffney, R. F. Garcia Ruiz, M. Godefroid, C. Granados, R. D. Harding, R. Heinke, M. Huyse, J. Karls, P. Larmonier, J. G. Li, K. M. Lynch, D. E. Maison, B. A. Marsh, P. Molkanov, P. Mosat, A. V. Oleynikenko, V. Pantelev, P. Pyykkö, M. L. Reitsma, K. Rezyunkina, R. E. Rossel, S. Rothe, J. Ruczkowski, S. Schiffmann, C. Seiffert, M. D. Seliverstov, S. Sels, L. V. Skripnikov, M. Stryczyk, D. Studer, M. Verlinde, S. Wilman, and A. V. Zaitsevskii, *Phys. Rev. Lett.* **127**, 192501 (2021).
- [8] R. An, X.-X. Dong, L.-G. Cao, and F.-S. Zhang, *Commun. Theor. Phys.* **75**, 035301 (2023).
- [9] M.-H. Mun, S. Kim, M.-K. Cheoun, W. So, S. Choi, and E. Ha, *Phys. Lett. B* **847**, 138298 (2023).
- [10] W. Nörtershäuser, D. Tiedemann, M. Žáková, Z. Andjelkovic, K. Blaum, M. L. Bissell, R. Cazan, G. W. F. Drake, C. Geppert, M. Kowalska, J. Krämer, A. Krieger, R. Neugart, R. Sánchez, F. Schmidt-Kaler, Z.-C. Yan, D. T. Yordanov, and C. Zimmermann, *Phys. Rev. Lett.* **102**, 062503 (2009).
- [11] W. Geithner, T. Neff, G. Audi, K. Blaum, P. Delahaye, H. Feldmeier, S. George, C. Guénaut, F. Herfurth, A. Herlert, S. Kappertz, M. Keim, A. Kellerbauer, H.-J. Kluge, M. Kowalska, P. Lievens, D. Lunney, K. Marinova, R. Neugart, L. Schweikhard, S. Wilbert, and C. Yazidjian, *Phys. Rev. Lett.* **101**, 252502 (2008).
- [12] S. Bagchi, R. Kanungo, W. Horiuchi, G. Hagen, T. Morris, S. Stroberg, T. Suzuki, F. Ameil, J. Atkinson, Y. Ayyad, D. Cortina-Gil, I. Dillmann, and A. Estradé, *Phys. Lett. B* **790**, 251 (2019).

- [13] S. Kaur, R. Kanungo, W. Horiuchi, G. Hagen, J. D. Holt, B. S. Hu, T. Miyagi, T. Suzuki, F. Ameil, J. Atkinson, Y. Ayyad, S. Bagchi, D. Cortina-Gil, I. Dillmann, A. Estradé, A. Evdokimov, F. Farinon, H. Geissel, G. Guastalla, R. Janik, R. Knöbel, J. Kurcewicz, Y. A. Litvinov, M. Marta, M. Mostazo, I. Mukha, C. Nociforo, H. J. Ong, T. Otsuka, S. Pietri, A. Prochazka, C. Scheidenberger, B. Sitar, P. Strmen, M. Takechi, J. Tanaka, I. Tanihata, S. Terashima, J. Vargas, H. Weick, and J. S. Winfield, *Phys. Rev. Lett.* **129**, 142502 (2022).
- [14] N. Wang and T. Li, *Phys. Rev. C* **88**, 011301(R) (2013).
- [15] B. A. Brown, *Phys. Rev. Lett.* **119**, 122502 (2017).
- [16] B. A. Brown, K. Minamisono, J. Piekarewicz, H. Hergert, D. Garand, A. Klose, K. König, J. D. Lantis, Y. Liu, B. Maaß, A. J. Miller, W. Nörtershäuser, S. V. Pineda, R. C. Powel, D. M. Rossi, F. Sommer, C. Sumithrarachchi, A. Teigelhöfer, J. Watkins, and R. Wirth, *Phys. Rev. Res.* **2**, 022035 (2020).
- [17] S. V. Pineda, K. König, D. M. Rossi, B. A. Brown, A. Incorvati, J. Lantis, K. Minamisono, W. Nörtershäuser, J. Piekarewicz, R. Powel, and F. Sommer, *Phys. Rev. Lett.* **127**, 182503 (2021).
- [18] S. J. Novario, D. Lonardonì, S. Gandolfi, and G. Hagen, *Phys. Rev. Lett.* **130**, 032501 (2023).
- [19] J.-Y. Xu, Z.-Z. Li, B.-H. Sun, Y.-F. Niu, X. Roca-Maza, H. Sagawa, and I. Tanihata, *Phys. Lett. B* **833**, 137333 (2022).
- [20] Y. N. Huang, Z. Z. Li, and Y. F. Niu, *Phys. Rev. C* **107**, 034319 (2023).
- [21] R. An, S. Sun, L.-G. Cao, and F.-S. Zhang, *Nucl. Sci. Tech.* **34**, 119 (2023).
- [22] P. Bano, S. P. Pattnaik, M. Centelles, X. Viñas, and T. R. Routray, *Phys. Rev. C* **108**, 015802 (2023).
- [23] K. König, J. C. Berengut, A. Borschevsky, A. Brinson, B. A. Brown, A. Dockery, S. Elhatisari, E. Eliav, R. F. G. Ruiz, J. D. Holt, B.-S. Hu, J. Kartheim, D. Lee, Y.-Z. Ma, U.-G. Meißner, K. Minamisono, A. V. Oley-nichenko, S. V. Pineda, S. D. Prosyak, M. L. Reitsma, L. V. Skripnikov, A. Vernon, and A. Zaitsevskii, *Phys. Rev. Lett.* **132**, 162502 (2024).
- [24] S. Gautam, A. Venneti, S. Banik, and B. Agrawal, *Nucl. Phys. A* **1043**, 122832 (2024).
- [25] I. Angeli and K. Marinova, *At. Data Nucl. Data Tables* **99**, 69 (2013).
- [26] T. Li, Y. Luo, and N. Wang, *At. Data Nucl. Data Tables* **140**, 101440 (2021).
- [27] A. Bohr and B. R. Mottelson, *Nuclear Structure* (World Scientific, Singapore, 1998).
- [28] S. Q. Zhang, J. Meng, S. G. Zhou, and J. Y. Zeng, *Eur. Phys. J. A* **13**, 285 (2002).
- [29] X.-X. Dong, R. An, J.-X. Lu, and L.-S. Geng, *Phys. Rev. C* **105**, 014308 (2022).
- [30] X.-X. Dong, R. An, J.-X. Lu, and L.-S. Geng, *Phys. Lett. B* **838**, 137726 (2023).
- [31] H. Nakada, *Phys. Rev. C* **100**, 044310 (2019).
- [32] R. Garcia Ruiz and A. Vernon, *Eur. Phys. J. A* **56**, 136 (2020).
- [33] A. J. Miller, K. Minamisono, A. Klose, D. Garand, C. Kujawa, J. D. Lantis, Y. Liu, B. Maaß, P. F. Mantica, W. Nazarewicz, W. Nörtershäuser, S. V. Pineda, P.-G. Reinhard, D. M. Rossi, F. Sommer, C. Sumithrarachchi, A. Teigelhöfer, and J. Watkins, *Nature Phys.* **15**, 432 (2019).
- [34] A. Huck, G. Klotz, A. Knipper, C. Miehé, C. Richard-Serre, G. Walter, A. Poves, H. L. Ravn, and G. Marguier, *Phys. Rev. C* **31**, 2226 (1985).
- [35] A. Gade, R. V. F. Janssens, D. Bazin, R. Broda, B. A. Brown, C. M. Campbell, M. P. Carpenter, J. M. Cook, A. N. Deacon, D.-C. Dinca, B. Fornal, S. J. Freeman, T. Glasmacher, P. G. Hansen, B. P. Kay, P. F. Mantica, W. F. Mueller, J. R. Terry, J. A. Tostevin, and S. Zhu, *Phys. Rev. C* **74**, 021302(R) (2006).
- [36] A. T. Gallant, J. C. Bale, T. Brunner, U. Chowdhury, S. Effenauer, A. Lennarz, D. Robertson, V. V. Simon, A. Chaudhuri, J. D. Holt, A. A. Kwiatkowski, E. Mané, J. Menéndez, B. E. Schultz, M. C. Simon, C. Andreoiu, P. Delheij, M. R. Pearson, H. Savajols, A. Schwenk, and J. Dilling, *Phys. Rev. Lett.* **109**, 032506 (2012).
- [37] F. Wienholtz, D. Beck, K. Blaum, C. Borgmann, M. Breitenfeldt, R. B. Cakirli, S. George, F. Herfurth, J. D. Holt, M. Kowalska, S. Kreim, D. Lunney, V. Manea, J. Menéndez, D. Neidherr, M. Rosenbusch, L. Schweikhard, A. Schwenk, J. Simonis, J. Stanja, R. N. Wolf, and K. Zuber, *Nature* **498**, 346 (2013).
- [38] R. F. Garcia Ruiz, M. L. Bissell, K. Blaum, A. Ekström, N. Frömmgen, G. Hagen, M. Hammen, K. Hebeler, J. D. Holt, G. R. Jansen, M. Kowalska, K. Kreim, W. Nazarewicz, R. Neugart, G. Neyens, W. Nörtershäuser, T. Papenbrock, J. Papuga, A. Schwenk, J. Simonis, K. A. Wendt, and D. T. Yordanov, *Nat. Phys.* **12**, 594 (2016).
- [39] A. Ekström, G. R. Jansen, K. A. Wendt, G. Hagen, T. Papenbrock, B. D. Carlsson, C. Forssén, M. Hjorth-Jensen, P. Navrátil, and W. Nazarewicz, *Phys. Rev. C* **91**, 051301 (2015).
- [40] K. Hebeler, S. K. Bogner, R. J. Furnstahl, A. Nogga, and A. Schwenk, *Phys. Rev. C* **83**, 031301 (2011).
- [41] L.-S. Geng, H. Toki, S. Sugimoto, and J. Meng, *Prog. Theor. Phys.* **110**, 921 (2003).
- [42] X. Xia, Y. Lim, P. Zhao, H. Liang, X. Qu, Y. Chen, H. Liu, L. Zhang, S. Zhang, Y. Kim, and J. Meng, *At. Data Nucl. Data Tables* **121-122**, 1 (2018).
- [43] K. Zhang, M.-K. Cheoun, Y.-B. Choi, P. S. Chong, J. Dong, Z. Dong, X. Du, L. Geng, E. Ha, X.-T. He, C. Heo, M. C. Ho, E. J. In, S. Kim, Y. Kim, C.-H. Lee, J. Lee, H. Li, Z. Li, T. Luo, J. Meng, M.-H. Mun, Z. Niu, C. Pan, P. Papakonstantinou, X. Shang, C. Shen, G. Shen, W. Sun, X.-X. Sun, C. K. Tam, Thaivayongnou, C. Wang, X. Wang, S. H. Wong, J. Wu, X. Wu, X. Xia, Y. Yan, R. W.-Y. Yeung, T. C. Yiu, S. Zhang, W. Zhang, X. Zhang, Q. Zhao, and S.-G. Zhou, *At. Data Nucl. Data Tables* **144**, 101488 (2022).
- [44] U. C. Perera, A. V. Afanasjev, and P. Ring, *Phys. Rev. C* **104**, 064313 (2021).
- [45] G. A. Lalazissis and S. E. Massen, *Phys. Rev. C* **53**, 1599 (1996).
- [46] G. Miller, A. Beck, S. May-Tal Beck, L. Weinstein, E. Piasetzky, and O. Hen, *Phys. Lett. B* **793**, 360 (2019).
- [47] L. A. Souza, M. Dutra, C. H. Lenzi, and O. Lourenço, *Phys. Rev. C* **101**, 065202 (2020).
- [48] W. Cosyn and J. Ryckebusch, *Phys. Lett. B* **820**, 136526 (2021).
- [49] R. An, L.-S. Geng, and S.-S. Zhang, *Phys. Rev. C* **102**, 024307 (2020).
- [50] R. An, X. Jiang, L.-G. Cao, and F.-S. Zhang, *Phys. Rev. C* **105**, 014325 (2022).

- [51] R. An, X. Jiang, N. Tang, L.-G. Cao, and F.-S. Zhang, (2023), [arXiv:2312.04912 \[nucl-th\]](#).
- [52] P.-G. Reinhard and W. Nazarewicz, *Phys. Rev. C* **95**, 064328 (2017).
- [53] S.-G. Zhou, J. Meng, and P. Ring, *Phys. Rev. C* **68**, 034323 (2003).
- [54] S.-G. Zhou, J. Meng, P. Ring, and E.-G. Zhao, *Phys. Rev. C* **82**, 011301 (2010).
- [55] X.-X. Sun, J. Zhao, and S.-G. Zhou, *Phys. Lett. B* **785**, 530 (2018).
- [56] K. Y. Zhang, P. Papakonstantinou, M.-H. Mun, Y. Kim, H. Yan, and X.-X. Sun, *Phys. Rev. C* **107**, L041303 (2023).
- [57] K. Zhang, S. Yang, J. An, S. Zhang, P. Papakonstantinou, M.-H. Mun, Y. Kim, and H. Yan, *Phys. Lett. B* **844**, 138112 (2023).
- [58] H. Liang, J. Meng, and S.-G. Zhou, *Phys. Rept.* **570**, 1 (2015).
- [59] R. Lisboa, P. Alberto, B. V. Carlson, and M. Malheiro, *Phys. Rev. C* **96**, 054306 (2017).
- [60] J. Geng, J. J. Li, W. H. Long, Y. F. Niu, and S. Y. Chang, *Phys. Rev. C* **100**, 051301 (2019).
- [61] Y.-T. Rong, P. Zhao, and S.-G. Zhou, *Phys. Lett. B* **807**, 135533 (2020).
- [62] N. Paar, P. Ring, T. Nikšić, and D. Vretenar, *Phys. Rev. C* **67**, 034312 (2003).
- [63] N. Paar, T. Nikšić, D. Vretenar, and P. Ring, *Phys. Rev. C* **69**, 054303 (2004).
- [64] S. S. Zhang, W. Zhang, S. G. Zhou, and J. Meng, *Eur. Phys. J. A* **32**, 43 (2007).
- [65] L.-G. Cao and Z.-Y. Ma, *Eur. Phys. J. A* **22**, 189 (2004).
- [66] S. Y. Chang, Z. H. Wang, Y. F. Niu, and W. H. Long, *Phys. Rev. C* **105**, 034330 (2022).
- [67] Z.-W. Lu, L. Guo, Z.-Z. Li, M. Ababekri, F.-Q. Chen, C. Fu, C. Lv, R. Xu, X. Kong, Y.-F. Niu, and J.-X. Li, *Phys. Rev. Lett.* **131**, 202502 (2023).
- [68] R. An, G.-F. Shen, S.-S. Zhang, and L.-S. Geng, *Chin. Phys. C* **44**, 074101 (2020).
- [69] C. Pan, K. Y. Zhang, P. S. Chong, C. Heo, M. C. Ho, J. Lee, Z. P. Li, W. Sun, C. K. Tam, S. H. Wong, R. W.-Y. Yeung, T. C. Yiu, and S. Q. Zhang, *Phys. Rev. C* **104**, 024331 (2021).
- [70] A. Ravlić, E. Yüksel, T. Nikšić, and N. Paar, *Phys. Rev. C* **108**, 054305 (2023).
- [71] Z. Li, S. Chen, M. Zhou, Y. Chen, and Z. Li, (2023), [arXiv:2309.03461 \[nucl-th\]](#).
- [72] D. D. Zhang, B. Li, D. Vretenar, T. Nikšić, Z. X. Ren, P. W. Zhao, and J. Meng, *Phys. Rev. C* **109**, 024316 (2024).
- [73] P. W. Zhao and S. Gandolfi, *Phys. Rev. C* **94**, 041302 (2016).
- [74] P. Ring, Y. K. Gambhir, and G. A. Lalazissis, *Comput. Phys. Commun.* **105**, 77 (1997).
- [75] G. A. Lalazissis, J. König, and P. Ring, *Phys. Rev. C* **55**, 540 (1997).
- [76] W. Long, J. Meng, N. V. Giai, and S.-G. Zhou, *Phys. Rev. C* **69**, 034319 (2004).
- [77] Y. K. Gambhir, P. Ring, and A. Thimet, *Ann. Phys.* **198**, 132 (1990).
- [78] M. Bender, P.-H. Heenen, and P.-G. Reinhard, *Rev. Mod. Phys.* **75**, 121 (2003).
- [79] D. Vretenar, A. Afanasjev, G. Lalazissis, and P. Ring, *Phys. Rept.* **409**, 101 (2005).
- [80] W. J. Huang, W. Meng., G. Audi, and S. Naimi, *Chin. Phys. C* **45**, 030002 (2021).
- [81] K. König, S. Fritzsche, G. Hagen, J. D. Holt, A. Klose, J. Lantis, Y. Liu, K. Minamisono, T. Miyagi, W. Nazarewicz, T. Papenbrock, S. V. Pineda, R. Powel, and P.-G. Reinhard, *Phys. Rev. Lett.* **131**, 102501 (2023).
- [82] J. Birkhan, M. Miorelli, S. Bacca, S. Bassauer, C. A. Bertulani, G. Hagen, H. Matsubara, P. von Neumann-Cosel, T. Papenbrock, N. Pietralla, V. Y. Ponomarev, A. Richter, A. Schwenk, and A. Tamii, *Phys. Rev. Lett.* **118**, 252501 (2017).
- [83] D. Adhikari, H. Albataineh, D. Androic, K. A. Aniol, D. S. Armstrong, T. Averett, C. Ayerbe Gayoso, S. K. Barcus, V. Bellini, R. S. Beminiwattha, J. F. Benesch, H. Bhatt, D. Bhatta Pathak, D. Bhetuwal, B. Blaikie, J. Boyd, Q. Campagna, A. Camsonne, G. D. Cates, Y. Chen, C. Clarke, J. C. Cornejo, S. Covrig Dusa, M. M. Dalton, P. Datta, A. Deshpande, D. Dutta, C. Feldman, E. Fuchey, C. Gal, D. Gaskell, T. Gautam, M. Gericke, C. Ghosh, I. Halilovic, J.-O. Hansen, O. Hassan, F. Hauenstein, W. Henry, C. J. Horowitz, C. Jantzi, S. Jian, S. Johnston, D. C. Jones, S. Kakkar, S. Katugampola, C. Keppel, P. M. King, D. E. King, K. S. Kumar, T. Kutz, N. Lashley-Colthirst, G. Leverick, H. Liu, N. Liyanage, J. Mammei, R. Mammei, M. McCaughan, D. McNulty, D. Meekins, C. Metts, R. Michaels, M. Mihovilovic, M. M. Mondal, J. Napolitano, A. Narayan, D. Nikolaev, V. Owen, C. Palatchi, J. Pan, B. Pandey, S. Park, K. D. Paschke, M. Petrusky, M. L. Pitt, S. Premathilake, B. Quinn, R. Radloff, S. Rahman, M. N. H. Rashad, A. Rathnayake, B. T. Reed, P. E. Reimer, R. Richards, S. Riordan, Y. R. Roblin, S. Seeds, A. Shahinyan, P. Souder, M. Thiel, Y. Tian, G. M. Urciuoli, E. W. Wertz, B. Wojtsekhowski, B. Yale, T. Ye, A. Yoon, W. Xiong, A. Zec, W. Zhang, J. Zhang, and X. Zheng (CREX Collaboration), *Phys. Rev. Lett.* **129**, 042501 (2022).
- [84] K. Oyamatsu, I. Tanihata, Y. Sugahara, K. Sumiyoshi, and H. Toki, *Nucl. Phys. A* **634**, 3 (1998).
- [85] B. Alex Brown, *Phys. Rev. Lett.* **85**, 5296 (2000).
- [86] R. J. Furnstahl, *Nucl. Phys. A* **706**, 85 (2002).
- [87] M. Warda, X. Viñas, X. Roca-Maza, and M. Centelles, *Phys. Rev. C* **80**, 024316 (2009).
- [88] M. Liu, Z.-X. Li, N. Wang, and F.-S. Zhang, *Chin. Phys. C* **35**, 629 (2011).
- [89] X. Roca-Maza, M. Centelles, X. Viñas, and M. Warda, *Phys. Rev. Lett.* **106**, 252501 (2011).
- [90] Z. Zhang and L.-W. Chen, *Phys. Lett. B* **726**, 234 (2013).
- [91] J. Xu, W.-J. Xie, and B.-A. Li, *Phys. Rev. C* **102**, 044316 (2020).
- [92] M. Warda, B. Nerlo-Pomorska, and K. Pomorski, *Nucl. Phys. A* **635**, 484 (1998).
- [93] A. Trzcińska, J. Jastrzębski, P. Lubiński, F. J. Hartmann, R. Schmidt, T. von Egidy, and B. Klos, *Phys. Rev. Lett.* **87**, 082501 (2001).
- [94] M. Warda, X. Viñas, X. Roca-Maza, and M. Centelles, *Phys. Rev. C* **81**, 054309 (2010).
- [95] M. Gaidarov, I. Moumène, A. Antonov, D. Kadrev, P. Sarriguren, and E. Moya de Guerra, *Nucl. Phys. A* **1004**, 122061 (2020).
- [96] S. Yoshida and H. Sagawa, *Phys. Rev. C* **69**, 024318 (2004).

- [97] T. Naito, T. Oishi, H. Sagawa, and Z. Wang, *Phys. Rev. C* **107**, 054307 (2023).
- [98] N. Wang, L. Ou, and M. Liu, *Phys. Rev. C* **87**, 034327 (2013).
- [99] M. Qiu, B.-J. Cai, L.-W. Chen, C.-X. Yuan, and Z. Zhang, *Phys. Lett. B* **849**, 138435 (2024).
- [100] M. M. Sharma, G. Lalazissis, J. König, and P. Ring, *Phys. Rev. Lett.* **74**, 3744 (1995).
- [101] J.-P. Ebran, A. Mutschler, E. Khan, and D. Vretenar, *Phys. Rev. C* **94**, 024304 (2016).
- [102] D. Zawischa, *Phys. Lett. B* **155**, 309 (1985).
- [103] J. Bishop, T. Kokalova, M. Freer, L. Acosta, M. Assié, S. Bailey, G. Cardella, N. Curtis, E. De Filippo, D. Dell'Aquila, S. De Luca, L. Francalanza, B. Gnoffo, G. Lanzalone, I. Lombardo, N. S. Martorana, S. Norella, A. Pagano, E. V. Pagano, M. Papa, S. Pirrone, G. Politi, F. Rizzo, P. Russotto, L. Quattrocchi, R. Smith, I. Stefan, A. Trifirò, M. Trimarchi, G. Verde, M. Vigilante, and C. Wheldon, *Phys. Rev. C* **100**, 034320 (2019).
- [104] S. Adachi, Y. Fujikawa, T. Kawabata, H. Akimune, T. Doi, T. Furuno, T. Harada, K. Inaba, S. Ishida, M. Itoh, C. Iwamoto, N. Kobayashi, Y. Maeda, Y. Matsuda, M. Murata, S. Okamoto, A. Sakaue, R. Sekiya, A. Tamii, and M. Tsumura, *Phys. Lett. B* **819**, 136411 (2021).
- [105] Z. H. Yang, Y. L. Ye, B. Zhou, H. Baba, R. J. Chen, Y. C. Ge, B. S. Hu, H. Hua, D. X. Jiang, M. Kimura, C. Li, K. A. Li, J. G. Li, Q. T. Li, X. Q. Li, Z. H. Li, J. L. Lou, M. Nishimura, H. Otsu, D. Y. Pang, W. L. Pu, R. Qiao, S. Sakaguchi, H. Sakurai, Y. Satou, Y. Togano, K. Tshoo, H. Wang, S. Wang, K. Wei, J. Xiao, F. R. Xu, X. F. Yang, K. Yoneda, H. B. You, and T. Zheng, *Phys. Rev. Lett.* **131**, 242501 (2023).
- [106] A. C. Dassie and R. M. I. Betan, *Phys. Rev. C* **108**, 044314 (2023).
- [107] B. Zhou, Y. Funaki, H. Horiuchi, Y.-G. Ma, G. Röpke, P. Schuck, A. Tohsaki, and T. Yamada, *Nature Commun.* **14**, 8206 (2023).
- [108] P.-G. Reinhard, W. Nazarewicz, and R. F. Garcia Ruiz, *Phys. Rev. C* **101**, 021301 (2020).
- [109] T. Naito, G. Colò, H. Liang, and X. Roca-Maza, *Phys. Rev. C* **104**, 024316 (2021).
- [110] T. Naito, X. Roca-Maza, G. Colò, H. Liang, and H. Sagawa, *Phys. Rev. C* **106**, L061306 (2022).
- [111] T. Naito, G. Colò, H. Liang, X. Roca-Maza, and H. Sagawa, *Phys. Rev. C* **107**, 064302 (2023).
- [112] P.-G. Reinhard and W. Nazarewicz, *Phys. Rev. C* **103**, 054310 (2021).
- [113] P.-G. Reinhard and W. Nazarewicz, *Phys. Rev. C* **105**, L021301 (2022).
- [114] R. An, S.-S. Zhang, L.-S. Geng, and F.-S. Zhang, *Chin. Phys. C* **46**, 054101 (2022).
- [115] J. Yang and J. Piekarewicz, *Phys. Rev. C* **97**, 014314 (2018).